Tryptophan-Mediated Interactions between Tristetraprolin and the CNOT9 Subunit Are Required for CCR4-NOT Deadenylase Complex Recruitment

Bulbrook, D.; Brazier, H.; Mahajan, P.; Kliszczak, M.; Fedorov, O.; Marchese, F. P.; Aubareda, A.; Chalk, R.; Picaud, S.; Strain-Damerell, C.; Filippakopoulos, P.; Gileadi, O.; Clark, A. R.; Yue, W.w.; Burgess-Brown, N. A.; Dean, J. L. E.

DOI:
10.1016/j.jmb.2017.12.018

Tryptophan-mediated interactions between tristetraprolin and the CNOT9 subunit are required for CCR4-NOT deadenylase complex recruitment

D. Bulbrook, H. Brazier, P. Mahajan, M. Kliszczak, O. Fedorov, F.P. Marchese, A. Aubareda, R. Chalk, S. Picaud, C. Strain-Damerell, P. Filippakopoulos, O. Gileadi, A.R. Clark, W.W. Yue, N.A. Burgess-Brown, J.L.E. Dean

PII: S0022-2836(17)30606-X
DOI: https://doi.org/10.1016/j.jmb.2017.12.018
Reference: YJMBI 65579

To appear in:

Received date: 26 July 2017
Revised date: 19 December 2017
Accepted date: 20 December 2017

Please cite this article as: D. Bulbrook, H. Brazier, P. Mahajan, M. Kliszczak, O. Fedorov, F.P. Marchese, A. Aubareda, R. Chalk, S. Picaud, C. Strain-Damerell, P. Filippakopoulos, O. Gileadi, A.R. Clark, W.W. Yue, N.A. Burgess-Brown, J.L.E. Dean , Tryptophan-mediated interactions between tristetraprolin and the CNOT9 subunit are required for CCR4-NOT deadenylase complex recruitment. The address for the corresponding author was captured as affiliation for all authors. Please check if appropriate. Yjmbi(2017), https://doi.org/10.1016/j.jmb.2017.12.018

Tryptophan-mediated interactions between tristetraprolin and the CNOT9 subunit are required for CCR4-NOT deadenylase complex recruitment

Bulbrook, D.[1¶], Brazier, H.[1,2¶], Mahajan, P.[2], Kliszczak, M.[2], Fedorov, O.[2], Marchese, F.P.[1], Aubareda, A.[1], Chalk, R.[2], Picaud, S.[2], Strain-Damerell, C.[2], Filippakopoulos, P.[2,3], Gileadi, O.[2], Clark, A.R.[4], Yue, W.W.[2]*, Burgess-Brown, N.A.[2]*, Dean, J.L.E.[1]*

¶ Equal contribution.

1. Kennedy Institute of Rheumatology, Nuffield Department of Orthopaedics, Rheumatology and Musculoskeletal Sciences, University of Oxford, Roosevelt Drive, Headington, Oxford, OX3 7FY, United Kingdom.

2. Structural Genomics Consortium, Nuffield Department of Clinical Medicine, University of Oxford, Old Road Campus Research Building, Roosevelt Drive, Headington, Oxford, OX3 7DQ, United Kingdom.

3. Ludwig Institute for Cancer Research, Old Road Campus Research Building, Roosevelt Drive, Oxford, OX3 7DQ, United Kingdom.

4. Institute of Inflammation and Ageing, University of Birmingham, Edgbaston, B15 2TT, United Kingdom.

* To whom correspondence should be addressed.

Tel: +44 (0)1954 210200; Fax: +44 (0)1954 210300; Email: jondean@cambio.co.uk

Tel: +44 (0)1865 617757; Fax: +44 (0)1865 617580; Email: wyatt.yue@sgc.ox.ac.uk

Tel: +44 (0)1865 617750; Fax: +44 (0)1865 617580; Email: nicola.burgess-brown@sgc.ox.ac.uk

Present address: Marchese, F.P, Center for Applied Medical Research, University of Navarra, 55 Pio XII Avenue, 31008 Pamplona, Spain. Aubareda, A., Department of Haematology, University of Cambridge, National Blood Service, Long Road, Cambridge CB2 2PT. Dean, J.L.E. Cambio Ltd, 1 The Irwin Centre, Scotland Road, Dry Drayton CB23 8AR.

Abstract

The zinc-finger protein tristetraprolin (TTP) binds to AU-rich elements present in the 3' untranslated regions of transcripts that mainly encode proteins of the inflammatory response. TTP-bound mRNAs are targeted for destruction via recruitment of the eight-subunit deadenylase complex 'carbon catabolite repressor protein 4 (CCR4) -negative on TATA-less (NOT)' which catalyzes the removal of mRNA poly-(A) tails, the first obligatory step in mRNA decay. Here we show that a novel interaction between TTP and the CCR4-NOT subunit, CNOT9, is required for recruitment of the deadenylase complex. In addition to CNOT1, CNOT9 is now included in the identified CCR4-NOT subunits shown to interact with TTP. We find that both the N- and C-terminal domains of TTP are involved in an interaction with CNOT9. Through a combination of SPOT peptide array, site-directed mutagenesis and bio-layer interferometry, we identified several conserved tryptophan (Trp) residues in TTP that serve as major sites of interaction with two Trp-binding pockets of CNOT9, previously found to interact with another modulator GW182. We further demonstrate that these interactions are also required for recruitment of the CCR4-NOT complex and TTP-directed decay of an mRNA containing an AU-rich element in its 3'-untranslated region. Together the results reveal new molecular details for the TTP-CNOT interaction that shape an emerging mechanism whereby TTP targets inflammatory mRNAs for deadenylation and decay.

Key words

Deadenylation; inflammatory; mRNA; AU-rich elements; post-translational control

Introduction

Tristetraprolin (TTP) is a 34 kDa RNA-binding zinc-finger protein that is expressed in a wide range of cell types including macrophages, dendritic cells, T-cells, endothelial cells, and fibroblasts [1]. TTP has been shown to be important for the induction and resolution of the expression of mRNAs of the inflammatory response and the proteins they encode. TTP binds to AU-rich elements (ARE) present in the 3'-untranslated regions (UTR) of its target mRNAs, directing them for degradation by promoting removal or shortening of poly-(A) tails, a process known as deadenylation, via the carbon catabolite

repressor protein 4 (CCR4) -negative on TATA-less (NOT) deadenylase complex [2, 3]. The importance of TTP in inflammation is demonstrated by the development of spontaneous inflammatory arthritis in TTP knockout ($TTP^{-/-}$) mice, which is primarily due to overexpression of tumor necrosis factor (TNF)-α [4]. Several hundreds of putative TTP-targeted mRNAs have been identified, mostly containing overlapping AUUUA repeats. Key TTP targets include mRNAs encoding TNF-α, cyclooxygenase-2, chemokine (C-X-C motif) ligand (CXCL)-1, CXCL-2, interleukin (IL)-1α, IL-1β and IL-10 as well as recently identified tissue factor [5-11].

The mechanism whereby TTP controls both the induction and resolution of inflammatory gene expression operates as follows. In cells that receive an inflammatory stimulus, or in chronic inflammation, the p38 mitogen-activated protein kinase (MAPK) pathway is activated, resulting in the induction of TTP mRNA and protein [12]. TTP protein is then phosphorylated by MAPK-activated protein kinase (MK2) [12, 13] at two major phosphorylation sites Ser-52 and Ser-178 (murine numbering) [13]. The consequence of TTP phosphorylation is two-fold: (i) it stabilizes TTP protein [14, 15] and promotes the binding of 14-3-3 to TTP [16], thereby localizing TTP in the cytoplasm [17, 18]; (ii) it prevents TTP from recruiting the CCR4-NOT deadenylase complex [2, 3], thereby inhibiting deadenylation, stabilizing inflammatory mRNAs, and increasing the translation of the proteins they encode. When signaling dissipates, TTP protein becomes dephosphorylated and activated, recruiting the CCR4-NOT complex to the mRNA which undergoes rapid deadenylation, and subsequent degradation [2, 3]. Dephosphorylation of TTP also expedites its proteasome-mediated decay [14], creating a window of time in which inflammatory mRNAs undergo decay before TTP protein itself is degraded. Thus, TTP not only participates in the induction and resolution of inflammatory gene expression, but the expression of TTP protein is also resolved, returning the cells to the resting state.

The function of TTP acting downstream of p38 MAPK and MK2 has been recently investigated using a murine knock-in (*ZFP36aa*) in which the two major MK2 phosphorylation sites in TTP, Ser-52 and Ser-178, were removed by serine to alanine mutagenesis [9]. The mice and macrophages isolated

from them display a profound impairment in the expression of not only TNF-α, but also several other inflammatory mRNAs and proteins, underscoring the importance of TTP and its phosphorylation in inflammation [9].

The CCR4-NOT deadenylase complex has a key function in the first obligatory step of mammalian mRNA decay, which triggers subsequent rapid degradation of the mRNA body. Therefore it controls the stability of a wide range of transcripts throughout the life cycle of mRNA. The human CCR4-NOT complex consists of eight stably-associated subunits [19] (Fig. 1). The core of the complex is the large scaffold protein CNOT1, decorated by six subunits that include a CNOT2:CNOT3 hetero-dimer [20], a CNOT10:CNOT11 hetero-dimer [21, 22], and a six-armadillo-repeat protein CNOT9. Two subunits with deadenylase activity are also bound by CNOT1, one being either CNOT6 (also called CCR4a) or CNOT6L (CCR4b), and the other being CNOT7 (CAF1a) or CNOT8 (CAF1b) [19]. In addition to the above eight subunits, an ubiquitin-dependent E3 ligase CNOT4 is weakly associated with the complex [19].

The relative arrangement and exact purpose of the CCR4-NOT subunits within the complex only begins to emerge from recent data, and remains unclear. CNOT2:CNOT3 interacts with CNOT1 via NOT boxes in the C-terminus of the proteins [20] [20]. CNOT10:CNOT11 have been suggested to bind to the N-terminal domain of CNOT1 [22], but little is known of their function. The armadillo repeats of CNOT9 fold into a crescent-shaped surface that binds to the middle domain of CNOT1 [23, 24]. How TTP recruits the deadenylase complex is also unclear. The 326-amino-acid human protein comprises three domains; both the N-terminal domain (NTD, aa 1-100) and C-terminal domain (CTD, aa 174-326) are largely unordered regions, shown to direct deadenylation and mRNA decay [25]. The central zing-finger domain (ZFD, aa 98-171) contains two zinc fingers for binding mRNA [26]. Recently, the TTP CTD [16] or the sequence spanning Ala-312 to Glu-326 of human TTP [27] have been shown to bind the CNOT1 subunit. However, the reported weak binding [27] suggests that additional binding sites on TTP, or interactions with CCR4-NOT subunits other than CNOT1, are important for TTP-directed deadenylation.

To this end, we hypothesized that TTP may recruit the CCR4-NOT complex additionally via the CNOT9 subunit. We predicted an interaction between conserved tryptophan (Trp) residues in TTP and Trp-binding pockets of CNOT9, based on report that in microRNA-mediated mRNA decay, these Trp-binding pockets of CNOT9 bind another modulator protein TNRC6/GW182 for recruitment of the RNA-induced silencing complex, RISC [23, 28]. In this study, we confirm that TTP indeed forms previously unreported interactions with the CNOT9 subunit involving conserved Trp residues, and that the Trp-mediated interactions are required for the recruitment of CCR4-NOT and ARE-mediated mRNA decay.

Results

Recombinant CNOT9 protein interacts directly with TTP

To understand how TTP recruits the CCR4-NOT complex, we aimed to determine if an analogous interaction to that occurring between GW182 of the RNA-induced silencing complex and the CNOT9 subunit, is formed between TTP and CNOT9. Pull-down assays with recombinantly-expressed His-CNOT9 (Fig. 2a) and GST-TTP were performed with immunodetection using anti-TTP and anti-His-tag antibodies. Full-length (FL) CNOT9 bound directly to FL GST-TTP (Fig. 2b, left). As negative control, recombinant His-CNOT10 protein (Fig. 2a), which is not known to interact with TTP, did not display any interaction with GST-TTP (Fig. 2b, right). As an orthogonal method to detect direct binding, bio-layer interferometry (BLI) has been utilized to measure the binding of biotinylated TTP (aa 14-326) towards CNOT9 and CNOT10. TTP binds CNOT9 strongly with micromolar affinity whereas little binding is detected against CNOT10 (Figure 2c).

Multiple regions of TTP are used to interact with CNOT9 protein

We next mapped the regions or domains of TTP involved in binding the CNOT9 subunit. Several truncated forms of human TTP encompassing different construct boundaries, all incorporated with an N-terminal His-tag for affinity purification and a C-terminal sequence for biotinylation in *E. coli* (Fig. 3a) were recombinantly produced. Each truncated TTP protein (Fig. 3c) was immobilized on

streptavidin sensors, and their binding to purified FL His-CNOT9 protein was analyzed by BLI (Fig. 3b, d). Near-FL TTP (aa 14-326) bound CNOT9 with a K_d of 5.5 $\pm$ 0.6 μM (Fig. 3b). The TTP NTD+ZFD protein without CTD (aa 14-171) also bound CNOT9 and displayed a similar K_d of 5.8 $\pm$ 1.2 μM. The TTP ZFD+CTD protein without NTD (aa 98-326) bound CNOT9 with a K_d of 9.6 ± 1.8 μM. Lastly, the ZFD-only TTP protein without NTD and CTD (aa 98-171) bound most weakly with a K_d of 17.3 ± 2.4 μM. BLI results therefore suggest that the entirety of the TTP sequence is involved in binding CNOT9, with the NTD contributing most to the interaction.

Tryptophan residues in TTP mediate CNOT9 binding

Since multiple regions of TTP are employed to interact with CNOT9, we aimed to define more closely the various sequence motifs involved. A SPOT peptide array of 15-mer overlapping peptides, covering the entire human TTP ORF (Fig. S2), was incubated with purified His-CNOT9 and probed with anti-His antibody. The intensity of immunoblotting for each SPOT peptide, an indicator of the strength of its binding to CNOT9, was plotted (Fig. 4a). Five sequence regions of the array (blue arrows), each represented by the peptide sequence of the intensity peak (peptides A04, B02, C04, D06, I01; arrows in Fig. 4a), displayed maximal CNOT9 binding. Among the five peak sequences, three of them contain Trp residues from either the NTD (Trp-32 and Trp-38 from peptide B02, Trp-69 from peptide C04) or the CTD (Trp-262 from peptide I01) (Fig. 4b). These Trp residues (Trp-32, Trp-38, Trp-69 and Trp-262) are strictly conserved across eukaryotic TTP sequences (Fig. S3). The Trp residues are clustered in Gly-Trp (GW)-like sequence motifs that are commonly employed in Agonaute-mediated interactions of gene silencing complexes [29]. Given the sequence conservation, the role of Trp containing motifs towards CNOT9 binding was validated by BLI using biotinylated TTP peptides (Fig. 4c). The peptides A04, C04 (encompassing Trp-69) and D06 did not bind in BLI. The peptide B02 (encompassing Trp-32 and Trp-38) bound to FL His-CNOT9 with a K_d of 56.5 ± 14.6 μM, while the peptide I01 (encompassing Trp-262) bound with a K_d of 9.3 ± 2.6 μM that represents a 5-fold increase in affinity compared to peptide B02 (Fig. 4c). Therefore, Trp-containing regions of TTP are important determinants for binding to CNOT9.

To confirm that the Trp residues in the TTP peptides directly contribute to interaction with CNOT9, an alanine-scanning array of peptides was generated where each amino acid in the peptides B02 and I01 was sequentially mutated to alanine (Fig. S3). This peptide array was probed with His-CNOT9 as before, and a drop in spot intensity of a mutated peptide, in comparison to the control wt spot, would indicate that the residue mutated is important for binding. As expected, peptides in which Trp-32, Trp-38, Trp-69 and Trp-262 were each substituted to alanine all exhibited reduced binding to CNOT9 (Fig. 5). Other residues were also found to reduce CNOT9 binding when mutated to alanine including Tyr7, Leu10, Leu11 in peptide A04. These were further investigated using synthesized biotinylated peptide, which was found not to bind CNOT9, and using an in vivo TTP recruitment assay, where mutation of YLL in TTP did not affect the ability of TTP to recruit the CCR4-NOT complex. Alanine substitutions for the four Trp residues (Trp-32, Trp-38, Trp-69 and Trp-262) were further carried out in the context of recombinant near-FL TTP expressed with a C-terminal biotin tag, and tested for CNOT9 binding by BLI as before (Fig. S4). In addition to single mutants (TTP W32A, TTP W38A, TTP W69A, TTP W262A), a quadruple mutant plasmid (TTP-4WA) was also constructed in which all four Trp residues in TTP were replaced with alanine (Fig. S4). The single Trp-to-Ala substitutions (TTP W32A, TTP W38A, TTP W262A) had no effect on CNOT9 binding response (Fig. 6a,c), with their K_ds similar to wt near-FL TTP (Fig. 6b). The W69A single mutant was not studied by BLI due to insoluble recombinant protein. Importantly, the TTP-4WA quadruple mutant displayed impaired binding for CNOT9 (Fig. 6a,c), which translated to an 8-fold higher K_d (81.4 ± 7.2 μM) than wt (10.3 ± 2.1 μM)(Fig. 6b).

Two tryptophan-binding pockets in CNOT9 are needed for interaction with TTP

We were interested in determining where in CNOT9 the TTP Trp residues bind. It is known that CNOT9 employs two Trp-binding pockets to interact with the GW motifs from other binding partners (e.g. GW182) [23, 28]. To investigate if a similar mechanism is also involved in interaction with TTP, key amino acid changes were made in either Trp-binding pocket 1 (CNOT9 P1; R205D, H208D) or 2

(CNOT9 P2; R244E, A248L) or in both pockets (CNOT9 P1+P2) of FL His-CNOT9 (Fig. S4). These residues were previously shown to form direct interactions with GW182 [23]. The wt and mutant CNOT9 proteins were assessed for binding biotinylated near-FL TTP in BLI (Fig. 7). Compared to wt CNOT9, mutations of either Trp-binding pocket (P1 or P2) or both (P1+P2) strongly interfered with the ability of CNOT9 protein to interact with near-FL TTP (Fig. 7). This effect is unlikely due to impairment of CNOT9 folding, as the mutant proteins behaved similarly to wt in size exclusion chromatography (Fig. S5) and have similar melting temperatures, as determined by differential scanning fluorimetry (DSF) (Fig. S6) [28], but instead likely due to the disruption of key interactions for the TTP Trp residues.

TTP-CNOT9 interaction is required for recruitment of the CCR4-NOT complex

We next determined if the TTP-CNOT9 interaction is relevant for recruitment of the intact CCR4-NOT complex. For this, mRNA for the CNOT9 subunit of the CCR4-NOT complex was efficiently depleted from HeLa cells (qRT-PCR, Fig. 8a) separately using two different siRNAs (CNOT9i and CNOT9ii) to control for off-target effects. Interactions between FL GST-mTTP or GST-alone control and the CCR4-NOT complex were assessed by pull-down assay. Interactions with CCR4-NOT were detected by immunoblotting for the CNOT2 subunit, thought to be stably associated with the CCR4-NOT complex and to not interact directly with the depleted CNOT9 subunit. Separate transfection of HeLa cells with the two different siRNAs targeting CNOT9 resulted in a reduction in TTP-bound CNOT2 subunit protein in GST-mTTP pull-downs (Fig. 8b), consistent with an interaction between CNOT9 and TTP.

FLAG-tagged TTP proteins corresponding to wt and the quadruple TTP-4WA mutant were expressed in HeLa tet-off cells, and immunoprecipitation was performed with anti-FLAG antibody agarose. CNOT2 and CNOT3 subunits were used for western analysis to assess recruitment of the entire CCR4-NOT complex to TTP. wt TTP co-immunoprecipitated with both CNOT2 and CNOT3 proteins, but interactions were not detected for the TTP-4WA mutant (Fig. 8c), and this was not due

to altered expression of CNOT2 and CNOT3 proteins in cells transfected with expression plasmid (Fig 8c). Therefore, Trp residues in TTP are required not only for its binding of CNOT9 using purified recombinant proteins, but also for the recruitment of intact CCR4-NOT complex in a crude cell extract.

Tryptophan to alanine substitutions in TTP inhibit TTP-directed ARE-mediated mRNA decay

We further investigated if the TTP-CNOT9 interaction is also functionally relevant for ARE-mediated mRNA decay. To do this, a HeLa cell line stably transfected with a plasmid bearing a tetracycline-sensitive transcription factor (HeLa tet-off) was used [30, 31]. These cells were transiently transfected with a plasmid expressing a reporter mRNA (BBB: rabbit beta-globin 5'UTR, beta-globin ORF, beta-globin 3'UTR) carrying 44 nucleotides of the TNF-α ARE inserted in its 3'UTR (BBB-TNF-ARE mRNA) [31]. The system allows transcription of the reporter mRNA in the absence of tetracycline. In control cells transfected with the reporter plasmid and carrier DNA (pBS), BBB-TNF-ARE mRNA was readily detected (Fig. 8d). Co-transfection of a wt TTP expression plasmid resulted in a reduction in BBB-TNF-ARE/GAPDH mRNA (Fig. 8d). On the contrary, the BBB-TNF-ARE/GAPDH mRNA level for co-transfected FLAG-TTP-4WA expression plasmid was 1.8-fold greater than that for wt TTP (Fig. 8d). Western blotting of cell lysates confirmed similar expression of FLAG-TTP-4WA and FLAG-TTP wt proteins (Fig. 8e). Therefore the Trp-to-Ala substitutions directly impacted on BBB-TNF-ARE steady-state levels.

Discussion

The CCR4-NOT deadenylase complex is a highly intricate, multi-protein machine that plays important roles in controlling gene expression, both by catalyzing the deadenylation of mRNAs leading to their subsequent degradation and also by controlling mRNA translation. Despite emerging details of the constituent subunits in the CCR4-NOT complex, its molecular architecture and protein-protein interactions, the mechanism of how it is recruited by TTP and how this interaction is regulated for the control of inflammatory gene expression remains poorly understood. To this end, we undertook a study aimed at identifying whether the CNOT9 subunit of the CCR4-NOT complex

directly interacts with TTP. Determining how such an interaction is formed may explain how TTP recruits the complex for control of inflammatory gene expression.

A GST pull-down assay identified CNOT9 as a novel interactor for the recruitment of TTP. siRNA-mediated depletion of the CNOT9 subunit corroborated this interaction using endogenous proteins. Using BLI and SPOT array analyses, the regions involved in the interaction with CNOT9 were mapped to multiple Trp residues present in the sequence of TTP. Crucially, alanine substitution of the four Trp residues in TTP significantly inhibited its ability to co-immunoprecipitate with the CCR4-NOT complex and impaired TTP-directed decay of an ARE-containing reporter mRNA. These results can be explained by the TTP-4WA mutant protein exhibiting an 8-fold weaker K_d for CNOT9 protein than wt TTP. Recruitment of the CCR4-NOT complex via Trp residues may therefore be a general mechanism, akin to the Trp residues in GW182 needed to bind CNOT9, for recruitment of the complex and miRNA-mediated control of gene expression [23, 28]. Thus, TTP-mediated mRNA decay and microRNA-mediated mRNA decay appear to utilize similar modes of protein-protein interactions.

Previous studies suggest the involvement of Trp residues in GW182 for recruitment of CNOT9 and the structures of CNOT9 soaked with Trp have identified two Trp-binding sites per CNOT9 subunit [23, 28]. We show here that the same two Trp-binding pockets in CNOT9 perform a similar binding function for four Trp residues in TTP. Only one CNOT9 subunit is present in the CCR4-NOT complex [23, 28] but CNOT9 also exists as a dimer when it is not associated with the complex [24]. Therefore one explanation may be that as many as four Trp residues in TTP may bind to the free CNOT9 dimer, but only two Trp residues to the single CNOT9 subunit found within the complex. Thus, the mode of TTP binding to CNOT9 may change following its recruitment to the complex. However, although human TTP contains four Trp residues, only three (Trp-32, Trp-38 and Trp-262) have been successfully validated here by mutational studies and BLI. Therefore, it may be that TTP is recruited to the CCR4-NOT complex by CNOT9 using Trp-32/38 and Trp-262 only.

Thus, in addition to the previously identified CNOT1 subunit [16, 27], CNOT9 also plays a key function in binding the CCR4-NOT complex for subsequent deadenylation of TTP-bound mRNA. At present, it is not entirely clear why two different CCR4-NOT subunits are needed for TTP to recruit the complex. One possible reason is that individual CNOT subunits bind TTP quite weakly. The extreme C-terminal sequence of TTP binds CNOT1 with a ~1 μM dissociation constant [27] and the TTP NTD and CTD constructs bind CNOT9 with a similar dissociation constant (for near-FL TTP K_d = 5.5 μM). It is also possible that TTP may interact with additional subunits of the CCR4-NOT complex, since multiple concerted interactions may promote formation of a sufficiently stable complex for deadenylation of TTP-bound target mRNAs. As TTP is known to have intrinsically disordered N- and C-termini, binding of one protein partner in the complex may induce secondary structure formation in a proximal domain of TTP, thus allowing another partner to bind. Binding of TTP to multiple subunits of the complex could therefore be co-operative to promote tighter binding. Multiple interactions may also be needed to correctly position TTP within the complex, in order for its cargo mRNA to be efficiently deadenylated.

In summary, we present a new interaction between TTP and the CCR4-NOT complex via CNOT9. We determine that TTP binds CNOT9 in a conserved Trp-mediated manner common to other CNOT9 binding partners. Given TTP's low affinity for CNOT9/CNOT1, it will be interesting to further explore the subunits for further TTP interactors. It will also be of interest in the future to design an artificial means of recruiting the CCR4-NOT complex that may offer an alternative to siRNA for the degradation of specific mRNAs in order to block gene expression, for use in the laboratory, or in a clinical setting.

Materials and Methods

Cloning

pGEX-6P-3-TTP and pGEX-6P-3-TTP-AA plasmids for expression of wt and S52/178A murine glutathione *S*-transferase (GST)-tagged forms of TTP protein in *E. coli* have been described

previously [2]. pGEX-6P-3-hTTP was constructed by restriction digest and ligation of the human TTP open reading frame (ORF) ((1-326) into the *Not* I site of pGEX-6P-3 (GE Healthcare). pNIC28-Bsa4-CNOT9 for expression in *E. coli* of 6xHis-tagged (His-) full-length human CNOT9 (1-299), pNH-TrxT-CNOT9 for 6xHis-thioredoxin (Trx)-tagged CNOT9 and pNIC28-Bsa4-CNOT3 for expression of His-CNOT3 (full-length human; 1-753) were constructed by ligation-independent cloning, using a high throughput PCR-based method utilizing the 3' → 5' exonuclease activity of T4 DNA polymerase to create overhangs with complementarity between the vector and insert [32]. The same method was used to generate pGTVL2-CNOT9 for expression of full-length CNOT9 protein (1-299) with N-terminal 6xHis and GST-tag. TTP proteins (aa 14-326, 98-326, 14-171, 98-171) were sub-cloned by ligation independent cloning into pNIC-Bio3, which provides an N-terminal 6xHis and a C-terminal biotin acceptor site [33]. CNOT9 mutant expression plasmids (mut P1 (pocket 1; R205D, H208D), mut P2 (pocket2; R244E, A248L) and mut P1+P2 (pockets 1+2; R205D, H208D, R244E, A248L)) were constructed using internal mutagenic and LIC primers following a primer extension method and sub-cloned into pNIC28-Bsa4 vector. The resulting mutant proteins bear N-terminal 6xHis-tags. TTP mutant protein expression plasmids encoding single mutants (TTP W32A, TTP W38A, TTP W69A, TTP W262A) or quadruple mutant TTP-4WA (W32A, W38A, W69A, W262A) were constructed as above. The mutants were sub-cloned into pNIC-Bio2 or pNIC28-Bio3 as to provide an N-terminal 6 or 10xHis-tag and a C-terminal biotin recognition sequence.

pCMV-FLAG-TTP-WT mammalian TTP protein expression plasmid was constructed by inserting the human TTP ORF (1-326) into pCMV-FLAG3 at the *Not* I site. This was mutagenized (GenScript) to produce pCMV-FLAG-TTP-4WA. pTetBBB-TNF-ARE has been previously described [31]. All plasmids used were sequence verified (Eurofins MWG Operon or Source BioScience).

Cell culture

HeLa cells (gift of Yamanouchi, Oxford, UK) were cultured in DMEM supplemented with 10 % (v/v) FCS and 1 % (v/v) penicillin/streptomycin and maintained by passaging at 37 °C in the presence of 5

% (v/v) CO_2. HeLa tet-Off cells (Clontech) were maintained as above but with the inclusion of 100 ng/ml G-418 (Life Technologies) in culture medium.

Transfection

HeLa cells were transfected with dsRNA (at a final concentration in culture medium of 15 nM) twice with a 24 h interval using Oligofectamine (Invitrogen) as previously described [34]. siRNAs used were in the *Silencer Select* range (Ambion). Scrambled dsRNA (Scr) 5'-CAGUCGCGUUUGCGACUGGdTdT-3' was used as a control (Eurofins MWG Operon). For reporter mRNA assays, HeLa tet-Off cells were transfected with plasmid DNA using Superfect (Qiagen) as previously described [30] with 100 ng of pTetBBB-TNF(44)ARE, with or without 50 ng of pCMV-FLAG-TTP expression plasmids and pBluescript (pBS) carrier plasmid DNA to a total of 1 μg of DNA per well of a six-well plate. For immunoprecipitations, each 10 cm dish was transfected with 0.4 μg pCMV-FLAG TTP expression plasmids and 7.6 μg pBS carrier DNA as above.

Purification of recombinant GST fusion proteins

This was performed as described previously [2] but using *E. coli* BL21(DE3)-R3-pRARE2 and expression of GST-fusion proteins was induced by addition of isopropyl 1-thio-β-D-galactopyranoside (IPTG) to 0.5 mM (final concentration) and cultures were incubated at 20 °C for 3 h before harvesting and purification.

Purification of recombinant His-tagged proteins

E. coli BL21(DE3)-R3-pRARE2 bacteria were transformed with expression plasmids by heat-shock. 1 L of terrific broth containing kanamycin (50 μg/ml) was inoculated with overnight culture, incubated at 37 ºC with shaking and allowed to reach OD_{600} of 1.4. IPTG was added to 0.1 mM (final concentration) and the culture was further incubated overnight at 18 ºC. Bacteria were harvested and resuspended in lysis buffer (100 mM HEPES (pH 7.6), 300 mM NaCl, 10 % (v/v) glycerol, 10 mM imidazole, 0.16 U/ml Benzonase, protease inhibitor cocktail). Homogenization was performed by

sonication and the homogenate clarified by centrifugation at 36,000 x g for 30 min. The clarified lysate was incubated with 1 ml (50 % (v/v) slurry) of Nickel Sepharose 6 FF (GE Healthcare) per 1 L of culture medium, equilibrated with lysis buffer with rotation for 1 h at 4 ºC. The resin was washed binding buffer (100 mM HEPES (pH 7.5), 300 mM NaCl, 10% (v/v) glycerol containing 20 mM imidazole) and wash buffer (containing 40 mM imidazole). Proteins were eluted using buffer containing 250 mM imidazole. For peptide arrays and BLI, CNOT9 protein was purified further by size exclusion chromatography (S200 16/600 on an ÄKTA system (GE Healthcare)) in 50 mM HEPES (pH 7.5), 300 mM NaCl, 0.5 mM TCEP, 5% (v/v) glycerol and concentrated to 4 mg/ml. His-tagged biotinylated proteins were expressed and purified as above with the following exceptions: *E. coli* BL21(DE3)-R3-pRARE2-BirA cultures containing kanamycin (50 µg/ml) and streptomycin (50 µg/ml) were grown to OD_{600} ~ 1.4 and induced as above with IPTG, but in the presence of 0.1 mM (final concentration) biotin and incubated overnight at 18 ºC. The final biotin concentration in the culture medium was increased to 0.2 mM and cultures incubated for a further hour before harvesting as above in lysis buffer containing 100 µM biotin. All purified His-tagged proteins were used immediately, or stored in aliquots at -80 ºC.

GST pull-down assay

HeLa cells were transfected with dsRNA, then 24 h later rinsed with ice-cold PBS and lyzed in 200 µl of a solution containing 10 mM HEPES (pH 7.6), 40 mM KCl, 3 mM $MgCl_2$, 2 mM DTT, 5 % (v/v) glycerol, 0.5 % (v/v) Igepal CA-630, 1 x Protease Inhibitor Cocktail (Calbiochem) for 10 min on ice and harvested by scraping. Samples were clarified by centrifugation at 100,000 x g at 4 ºC for 10 min. 300 µg of HeLa cell extract was incubated with 2 µg of GST-TTP and 40 µl of a 50 % (v/v) slurry of Glutathione Sepharose 4B in 1 ml of binding buffer (10 mM HEPES (pH 7.6), 100 mM KCl, 6 mM $MgCl_2$, 1 mM DTT, 1 % (v/v) Igepal CA-360) for 1 h at 4 °C with rotation. The glutathione-agarose beads were centrifuged at 6 200 x g for 1 min and washed three times with 1 ml of binding buffer, centrifuging at each stage as above. The beads were aspirated to dryness and incubated in 40 µl SDS-PAGE sample buffer (60 mM Tris-HCl pH (6.8), 2 % (w/v) SDS, 10 % (v/v) glycerol, 0.025 % (w/v)

bromophenol blue) at 95 °C for 5 min. The supernatant was loaded on a SDS-polyacrylamide gel, and following electrophoresis, proteins were analyzed by western blotting. For GST pull-down assays using purified recombinant proteins, an identical procedure was followed except that binding was performed with 1 µg of GST-TTP and 1 µg of His-tagged recombinant protein.

Bio-Layer Interferometry

BLI experiments were performed on a 16-channel ForteBio Octet RED384 instrument at 25 °C. Measurements were performed in the same gel filtration buffers used to purify CNOT9 protein. C-terminal biotinylated TTP protein or C- or N-terminal-biotinylated TTP-derived peptides were attached to streptavidin coated biosensors (super-streptavidin, SSA) by incubating for 6 min at a concentration of 3 µM. For measurements to determine K_d, His-CNOT9 sample was prepared in seven 2.0 fold dilutions starting from 20 µM (TTP NTD+ZFD) or 80 µM (near-FL TTP). Wild type His-CNOT9 protein and Trp pocket mutant forms were used at 20 µM in conjunction with TTP near-FL protein. Measurements were performed using a 180 sec association step followed by a 180 sec dissociation step on a black 384-well plate with tilted bottom (ForteBio). The baseline was stabilized for 120 sec prior to association and signal from the reference sensors was subtracted prior to K_d calculations using GraphPad Prism (GraphPad Software). The change in wavelength (nm), measured for each concentration of CNOT9, was plotted against CNOT9 concentration. This plot was used to derive the Kd of CNOT9 for each TTP construct using GraphPad prism and the following equation for a one site total binding model.

$$Y = \frac{Bmax\ X}{(Kd+X)} + NS*X + Background$$

Where Bmax is the maximum specific binding in the same units as Y. Kd is the equilibrium binding constant. NS is the slope of non-specific binding in Y units divided by X units. Background is the amount of non-specific binding with no added substrate.

SPOT Peptide Assays

Cellulose-bound peptide arrays were prepared according to standard protocols using a MultiPep-RSi-Spotter (INTAVIS, Köln, Germany) employing Fmoc solid phase peptide SPOT synthesis according to the manufacturer's instructions. Human TTP peptides (using UniProt accession code P26651) were synthesized on Amino-PEG500-UC540 Sheets optimized for use with the MultiPep instruments (INTAVIS); the presence of SPOTted peptides was confirmed by ultraviolet light (UV, λ = 280 nM). Membranes were blocked with 5 % (w/v) bovine serum albumin (Fisher Scientific) overnight then incubated overnight with His-tagged recombinant CNOT9 at 4 ˚C. After washing with PBS-T buffer (3.2 mM Na_2HPO_4, 0.5 mM KH_2PO_4, (pH7.4), 1.3 mM KCl, 135 mM NaCl and 0.1 % (v/v) Tween 20) to remove any unbound material, bound protein was detected using horse radish peroxidase-conjugated anti-His antibody (Novagene) and the Pierce® ECL Western blotting Substrate (Thermo Scientific). Chemiluminescence was detected with an image reader (Fujifilm LAS-4000 ver.2.0) typically using an incremental exposure time of 5 min for a total of 80 min (or until saturation was reached, in the case of very strong signal). Peptide locations on the array and their sequences are given in Supplementary Table 1.

Immunoprecipitation

Cells were harvested 24 h post-transfection and lysed in 50 mM Tris-HCl (pH 7.5), 150 mM KCl, 3 mM $MgCl_2$, 5 % (v/v) glycerol, 0.5 % (v/v) Igepal CA-630, 1 x Protease Inhibitor cocktail and lysates were incubated with anti-FLAG M2 agarose (Sigma-Aldrich) for 16 h on a rotating wheel at 4 °C. The beads were washed five times with 50 mM Tris-HCl (pH 7.5), 150 mM NaCl, boiled in SDS-PAGE sample buffer for 5 min and eluted proteins analyzed by western blotting.

qRT-PCR

RNA was isolated using an RNeasy kit (Qiagen) and cDNA generated with a Reverse Transcription-PCR kit (Ambion Life Technologies) according to the manufacturers' instructions. cDNA was analyzed by real-time PCR using TaqMan primer-probe sets (Applied Biosystems). A ViiA 7 Real-Time PCR system (Applied Biosystems) or a Rotor-Gene 6000 thermal cycler (Corbett) and

associated software for the $\Delta\Delta C_t$ method of relative quantitation (with standard curves) were used to quantify mRNAs with normalization to GAPDH mRNA.

BBB-ARE mRNA reporter assay

24 h post-transfection cells were harvested and RNA was isolated as above but with an on-column DNase I (Qiagen) digestion step to remove plasmid DNA and qRT-PCR performed with β-globin and GAPDH mRNA Taqman primer-probe sets (Applied Biosystems).

SDS-PAGE and western blotting

SDS-PAGE was performed according to standard procedures. For experiments employing siRNA or immunoprecipitation, proteins were separated on 10 % polyacrylamide-SDS gels using a Tris-glycine buffer system. For other experiments, pre-cast NuPAGE 4-12 % gradient gels (Novex) were used. For western blotting, proteins were transferred to a PVDF membrane, visualized with Coomassie Blue R-250, destained with methanol, and detected with the following primary antibodies: SAK21 antibody raised in rabbits against a C-terminal TTP peptide [12]; anti-CNOT2 (Bethyl Laboratories); anti-CNOT3 (Bethyl Laboratories); anti-α-tubulin (Sigma-Aldrich); anti-His-tag (Millipore); anti-GAPDH (Sigma Aldrich). Horse radish peroxidase-conjugated secondary antibodies (DAKO) were used in combination with the enhanced chemiluminescence system (GE Healthcare).

Measurement of protein concentration

Concentrations of purified recombinant proteins were determined by measuring A_{280} using a Nanodrop 1000 spectrophotometer (Thermoscientific) and using extinction coefficients calculated with ExPASy ProtParam tool (http://web.expasy.org/protparam/). Protein concentrations of HeLa cell lysates were estimated according to Bradford [35] using a BSA standard curve and a BioPhotometer (Eppendorf).

Acknowledgements

We are grateful to Alex Bullock, Jon Elkins, Benedikt Kessler, Jeremy Saklatvala, Chris Norbury and Irina Udalova for their useful suggestions.

Funding

This work was supported by The Kennedy Trust for Rheumatology Research (MSP 10/11 05; MSP 12/13 01) and an Arthritis Research UK grant (17551). The Structural Genomics Consortium is a registered charity (number 1097737) that receives funds from AbbVie, Bayer Pharma AG, Boehringer Ingelheim, Canada Foundation for Innovation, Eshelman Institute for Innovation, Genome Canada, Innovative Medicines Initiative (EU/EFPIA) [ULTRA-DD grant no. 115766], Janssen, Merck & Co., Novartis Pharma AG, Ontario Ministry of Economic Development and Innovation, Pfizer, São Paulo Research Foundation-FAPESP, Takeda, and Wellcome Trust [092809/Z/10/Z]. S.P. and P.F. are supported by a Wellcome Career Development Fellowship (095751/Z/11/Z).

References

[1] Brooks SA, Blackshear PJ. Tristetraprolin (TTP): interactions with mRNA and proteins, and current thoughts on mechanisms of action. Biochimica et biophysica acta. 2013;1829:666-79.

[2] Marchese FP, Aubareda A, Tudor C, Saklatvala J, Clark AR, Dean JL. MAPKAP kinase 2 blocks tristetraprolin-directed mRNA decay by inhibiting CAF1 deadenylase recruitment. The Journal of biological chemistry. 2010;285:27590-600.

[3] Clement SL, Scheckel C, Stoecklin G, Lykke-Andersen J. Phosphorylation of tristetraprolin by MK2 impairs AU-rich element mRNA decay by preventing deadenylase recruitment. Mol Cell Biol. 2011;31:256-66.

[4] Taylor GA, Carballo E, Lee DM, Lai WS, Thompson MJ, Patel DD, et al. A pathogenetic role for TNF alpha in the syndrome of cachexia, arthritis, and autoimmunity resulting from tristetraprolin (TTP) deficiency. Immunity. 1996;4:445-54.

[5] Carballo E, Lai WS, Blackshear PJ. Feedback inhibition of macrophage tumor necrosis factor-alpha production by tristetraprolin. Science. 1998;281:1001-5.

[6] Datta S, Biswas R, Novotny M, Pavicic PG, Jr., Herjan T, Mandal P, et al. Tristetraprolin regulates CXCL1 (KC) mRNA stability. J Immunol. 2008;180:2545-52.

[7] Stoecklin G, Tenenbaum SA, Mayo T, Chittur SV, George AD, Baroni TE, et al. Genome-wide analysis identifies interleukin-10 mRNA as target of tristetraprolin. J Biol Chem. 2008;283:11689-99.

[8] Tudor C, Marchese FP, Hitti E, Aubareda A, Rawlinson L, Gaestel M, et al. The p38 MAPK pathway inhibits tristetraprolin-directed decay of interleukin-10 and pro-inflammatory mediator mRNAs in murine macrophages. FEBS letters. 2009;583:1933-8.

[9] Ross EA, Smallie T, Ding Q, O'Neil JD, Cunliffe HE, Tang T, et al. Dominant Suppression of Inflammation via Targeted Mutation of the mRNA Destabilizing Protein Tristetraprolin. J Immunol. 2015;195:265-76.

[10] Iqbal MB, Johns M, Cao J, Liu Y, Yu SC, Hyde GD, et al. PARP-14 combines with tristetraprolin in the selective posttranscriptional control of macrophage tissue factor expression. Blood. 2014;124:3646-55.

[11] Kratochvill F, Machacek C, Vogl C, Ebner F, Sedlyarov V, Gruber AR, et al. Tristetraprolin-driven regulatory circuit controls quality and timing of mRNA decay in inflammation. Mol Syst Biol. 2011;7:560.

[12] Mahtani KR, Brook M, Dean JL, Sully G, Saklatvala J, Clark AR. Mitogen-activated protein kinase p38 controls the expression and posttranslational modification of tristetraprolin, a regulator of tumor necrosis factor alpha mRNA stability. Mol Cell Biol. 2001;21:6461-9.

[13] Chrestensen CA, Schroeder MJ, Shabanowitz J, Hunt DF, Pelo JW, Worthington MT, et al. MAPKAP kinase 2 phosphorylates tristetraprolin on in vivo sites including Ser178, a site required for 14-3-3 binding. J Biol Chem. 2004;279:10176-84.

[14] Brook M, Tchen CR, Santalucia T, McIlrath J, Arthur JS, Saklatvala J, et al. Posttranslational regulation of tristetraprolin subcellular localization and protein stability by p38 mitogen-activated protein kinase and extracellular signal-regulated kinase pathways. Mol Cell Biol. 2006;26:2408-18.

[15] Hitti E, Iakovleva T, Brook M, Deppenmeier S, Gruber AD, Radzioch D, et al. Mitogen-activated protein kinase-activated protein kinase 2 regulates tumor necrosis factor mRNA stability and

translation mainly by altering tristetraprolin expression, stability, and binding to adenine/uridine-rich element. Mol Cell Biol. 2006;26:2399-407.

[16] Sandler H, Kreth J, Timmers HT, Stoecklin G. Not1 mediates recruitment of the deadenylase Caf1 to mRNAs targeted for degradation by tristetraprolin. Nucleic Acids Res. 2011.

[17] Johnson BA, Stehn JR, Yaffe MB, Blackwell TK. Cytoplasmic localization of tristetraprolin involves 14-3-3-dependent and -independent mechanisms. J Biol Chem. 2002;277:18029-36.

[18] Stoecklin G, Stubbs T, Kedersha N, Wax S, Rigby WF, Blackwell TK, et al. MK2-induced tristetraprolin:14-3-3 complexes prevent stress granule association and ARE-mRNA decay. EMBO J. 2004;23:1313-24.

[19] Lau NC, Kolkman A, van Schaik FM, Mulder KW, Pijnappel WW, Heck AJ, et al. Human Ccr4-Not complexes contain variable deadenylase subunits. Biochem J. 2009;422:443-53.

[20] Boland A, Chen Y, Raisch T, Jonas S, Kuzuoglu-Ozturk D, Wohlbold L, et al. Structure and assembly of the NOT module of the human CCR4-NOT complex. Nat Struct Mol Biol. 2013;20:1289-97.

[21] Bawankar P, Loh B, Wohlbold L, Schmidt S, Izaurralde E. NOT10 and C2orf29/NOT11 form a conserved module of the CCR4-NOT complex that docks onto the NOT1 N-terminal domain. RNA Biol. 2013;10:228-44.

[22] Mauxion F, Preve B, Seraphin B. C2ORF29/CNOT11 and CNOT10 form a new module of the CCR4-NOT complex. RNA Biol. 2013;10:267-76.

[23] Mathys H, Basquin J, Ozgur S, Czarnocki-Cieciura M, Bonneau F, Aartse A, et al. Structural and Biochemical Insights to the Role of the CCR4-NOT Complex and DDX6 ATPase in MicroRNA Repression. Mol Cell. 2014.

[24] Garces RG, Gillon W, Pai EF. Atomic model of human Rcd-1 reveals an armadillo-like-repeat protein with in vitro nucleic acid binding properties. Protein Sci. 2007;16:176-88.

[25] Lykke-Andersen J, Wagner E. Recruitment and activation of mRNA decay enzymes by two ARE-mediated decay activation domains in the proteins TTP and BRF-1. Genes Dev. 2005;19:351-61.

[26] Lai WS, Carballo E, Strum JR, Kennington EA, Phillips RS, Blackshear PJ. Evidence that tristetraprolin binds to AU-rich elements and promotes the deadenylation and destabilization of tumor necrosis factor alpha mRNA. Mol Cell Biol. 1999;19:4311-23.

[27] Fabian MR, Frank F, Rouya C, Siddiqui N, Lai WS, Karetnikov A, et al. Structural basis for the recruitment of the human CCR4-NOT deadenylase complex by tristetraprolin. Nature structural & molecular biology. 2013;20:735-9.

[28] Chen Y, Boland A, Kuzuoglu-Ozturk D, Bawankar P, Loh B, Chang CT, et al. A DDX6-CNOT1 Complex and W-Binding Pockets in CNOT9 Reveal Direct Links between miRNA Target Recognition and Silencing. Mol Cell. 2014.

[29] Pfaff J, Meister G. Argonaute and GW182 proteins: an effective alliance in gene silencing. Biochem Soc Trans. 2013;41:855-60.

[30] Lasa M, Mahtani KR, Finch A, Brewer G, Saklatvala J, Clark AR. Regulation of cyclooxygenase 2 mRNA stability by the mitogen-activated protein kinase p38 signaling cascade. Mol Cell Biol. 2000;20:4265-74.

[31] Dean JL, Wait R, Mahtani KR, Sully G, Clark AR, Saklatvala J. The 3' Untranslated Region of Tumor Necrosis Factor Alpha mRNA Is a Target of the mRNA-Stabilizing Factor HuR. Mol Cell Biol. 2001;21:721-30.

[32] Savitsky P, Bray J, Cooper CD, Marsden BD, Mahajan P, Burgess-Brown NA, et al. High-throughput production of human proteins for crystallization: the SGC experience. J Struct Biol. 2010;172:3-13.

[33] Keates T, Cooper CD, Savitsky P, Allerston CK, Phillips C, Hammarstrom M, et al. Expressing the human proteome for affinity proteomics: optimising expression of soluble protein domains and in vivo biotinylation. N Biotechnol. 2012;29:515-25.

[34] Alford KA, Glennie S, Turrell BR, Rawlinson L, Saklatvala J, Dean JL. Heat shock protein 27 functions in inflammatory gene expression and transforming growth factor-beta-activated kinase-1 (TAK1)-mediated signaling. J Biol Chem. 2007;282:6232-41.

[35] Bradford MM. A rapid and sensitive method for the quantitation of microgram quantities of protein utilizing the principle of protein-dye binding. Anal Biochem. 1976;72:248-54.

Figure Legends

Figure 1. Diagram of the CCR4-NOT complex and interacting subunits.

The CCR4-NOT complex is an eight-subunit multi-protein complex comprised of CNOT1, which forms the main scaffolding protein onto which docks CNOT2-11. CNOT6/6L and CNOT7/8 are mutually exclusive catalytic subunits which deadenylate mRNAs. TTP, an RNA-binding protein, recruits the complex which brings together inflammatory mRNAs bound by TTP and deadenylase subunits of the CCR4-NOT complex as a mechanism of mRNA decay. It is known that TTP is recruited to the complex by an interaction between the C-terminus of TTP and a central domain of CNOT1. It is unknown if there are further interactions between TTP and other CNOT subunits, highlighted by question marks.

Figure 2. CNOT9 is a novel TTP-interacting subunit of the CCR4-NOT complex.

a, Schematic depicting recombinant His-CNOT9 and His-CNOT3. The CNOT9 armadillo repeat (Arm Repeat) region is highlighted in pink, the CNOT3 NOT box is highlighted in orange, the His-tag is shown in green and additional regions of the ORFs are shown in grey. Amino acid boundaries are indicated. b, recombinant His-CNOT9 or His-CNOT10 proteins were incubated with GST-TTP or GST (control) and pulled-down proteins were analysed by western blot with anti-His and anti-TTP antibodies. Similar results were seen in three separate experiments. Positions of markers (Mol. mass (kDa)) are shown. c. Concentration vs change in wavelength ($\Delta\ \lambda$ nm) plots from BLI experiment to determine interactions between TTP and CNOT9/CNOT10, over a range of CNOT9/CNOT10 concentrations (μM).

Figure 3. Identification of domains in TTP that mediate CNOT9 protein binding

a, Schematic showing truncated His- (dark green), Trx- (blue) and biotin- (dark blue) TTP used to assess function of domains in CNOT9 binding (FL, full-length; near-FL, near full-length; NTD, N-terminal domain (orange); ZFD, zinc finger domain (pink); CTD, C-terminal domain (green)). b, Table of dissociation constants ($K_{d,}$ μM) of TTP near-FL, TTP NTD+ZFD, CTD+ZFD and ZFD

binding to CNOT9 protein. c, Left: Streptavidin-mediated affinity purification of TTP domains (aa 14-171, aa 98-326 and aa 14-326); right: Post-affinity purification sample of TTP zinc-finger domain-only protein (aa 98-171). d, Concentration vs change in wavelength (Δ λ nm) plots for TTP domains. Interactions between TTP domains and CNOT9 was measured using BLI at a range of CNOT9 concentrations (μM). The change in wavelength, as measured by BLI, has been plotted against CNOT9 concentration using GraphPad prism. The plots were fitted using a one site total binding model and the binding affinities were calculated using GraphPad.

Figure 4. SPOT peptide array identifying tryptophan residues in TTP that mediate CNOT9 binding

TTP peptide array was probed with recombinant His-CNOT9 protein and binding detected using an anti-His antibody and chemiluminescence. a, Plot of Intensity (% of max.) of chemiluminescence signal for His-CNOT9 protein binding to TTP peptides. Blue arrows indicate peptides which show a peak of CNOT9 binding. b, The amino acid sequence of the TTP ORF is shown. Conserved tryptophan residues are shown in bold red type. The sequence of each peptide identified from the intensity plot is underlined and the peptide identifier (A04, B02, C04, D06, I01) is given above. The amino acid position of each tryptophan residue is shown in grey text underneath each peptide. c, Binding of peptides was validated using BLI. Table shows binding constants (K_d, μM) calculated using wavelength shift (Δλ) response (nm) against time for binding and dissociation of biotin-tagged wt TTP peptides immobilised on the streptavidin sensor to wt CNOT9.

Figure 5. Multiple tryptophan residues in TTP contribute to CNOT9 binding

The intensities of the spots in the alanine scanning TTP peptide array were measured and calculated as a percentage of the intensity of the wt peptide in the series. The percentage intensities of each peptide in the series have been plotted in bar graphs and the corresponding spots overlaid above the graph. The identification of each peptide is listed above each graph. Each bar has been labelled with the residue and amino acid position number which has been mutated to alanine. A drop in percentage

intensity indicates the mutated residue is important for binding CNOT9. When mutated to alanine, a number of tryptophan residues show decreased binding (bold), indicating their importance.

Figure 6. TTP tryptophan residues are involved in CNOT9 binding

a, Plot showing responses in BLI (nm) against time for binding of immobilized near-FL wt and mutant TTP (W32A, W38A, W262A and 4WA) to wt CNOT9 protein. Results are representative of two independent experiments. b, Table shows binding constants (K_d, μM) calculated using wavelength shift (Δλ) response (nm) against time for binding and dissociation of biotin-tagged wt TTP, W32A, W38A, W262A and TTP-4WA quadruple mutant immobilized on the streptavidin sensor to CNOT9 protein. c, Concentration vs change in wavelength (Δ λ nm) plots for TTP wt and mutants. Interactions between TTP wt/mutants and CNOT9 was measured using BLI at a range of CNOT9 concentrations (μM). The change in wavelength, as measured by BLI, has been plotted against CNOT9 concentration using GraphPad prism. The plots were fitted using a one site total-binding model and the binding affinities were calculated using GraphPad.

Figure 7. Tryptophan-binding pockets in CNOT9 are needed for TTP binding

a, Plot showing responses in BLI (nm) against time for binding of immobilized TTP near-FL to wt CNOT9 protein and mutant forms (CNOT9 P1 (R205D, H208D), CNOT9 P2 (R244E, A248L) and CNOT9 P1+P2 (R205D, H208D, R244E, A248L). Results are representative of two independent experiments. b, Table shows binding constants (K_d, μM) calculated using wavelength shift (Δλ) response (nm) against time for binding and dissociation of biotin-tagged wt TTP immobilized on the streptavidin sensor to wt CNOT9 and P1, P2 and P1+P2 mutant CNOT9 protein. c, Concentration vs change in wavelength (Δ λ nm) plots for CNOT9 wt and mutants. Interactions between CNOT9 wt/mutants and TTP wt was measured using BLI at a range of CNOT9 concentrations (μM). The change in wavelength, as measured by BLI, has been plotted against CNOT9 concentration using GraphPad prism. The plots were fitted using a one site total-binding model and the binding affinities were calculated using GraphPad.

Figure 8. Tryptophan residues in TTP are needed for interactions with the CCR4-NOT complex and for TTP-directed mRNA decay.

a, , HeLa cells were transfected separately with a scrambled control dsRNA (Scr) or two siRNAs targeting CNOT9 (CNOT9i and CNOT9ii). CNOT9 and GAPDH mRNAs were quantified by qRT-PCR (as indicated) for duplicate wells of cells. Plots show mean (and SD) CNOT9/GAPDH mRNA (normalized to Scr) for 2 experiments performed in duplicate. B, Additional duplicates of cells transfected in (A) were lysed and pull-down performed with GST (as a control) or GST-mTTP protein. Pulled-down proteins and input lysates (INPUT) were analyzed by western blot for CNOT2, TTP and α-tubulin (as a loading control) as indicated. Results shown are representative of two independent experiments. c, Western blot of anti-FLAG antibody immunoprecipitation. HeLa tet-off cells were transfected in 10 cm dishes with carrier pBluescript (pBS) DNA (as a control) or with pCMV-FLAG-TTP-WT (wt hTTP) or pCMV-FLAG-TTP-4WA (TTP with all four tryptophans substituted for alanines) expression plasmids. Western blot was performed with cell lysates (0.1 or 5% INPUT as indicated) or immunoprecipitated proteins for CNOT3, CNOT2, TTP and GAPDH. d, RNA from cells transfected as in (C) but in 6 well plates together with pTet-BBB-TNF-ARE was analyzed by qRT-PCR for β-globin and GAPDH mRNAs. Graph shows mean and S.E.M. for BBB-TNF-ARE/GAPDH mRNA from two independent experiments performed in duplicate (unpaired Student's t test: **** $P < 0.0001$; *** $P < 0.001$; ** $P < 0.01$). e, Western blot of lysates from cells transfected in duplicate (1,2) in (D) showing expression levels of FLAG-TTP proteins and GAPDH protein.

Highlights

- **TTP targets inflammatory mRNA for degradation by interacting with CCR4-CNOT complex**
- **We identified one subunit of the complex, CNOT9, as a novel interactor of TTP**
- **TTP binds using conserved Trp residues to CNOT9 regions common to other modulators**
- **Trp-mediated interactions with CNOT9 are essential to TTP-mediated decay**

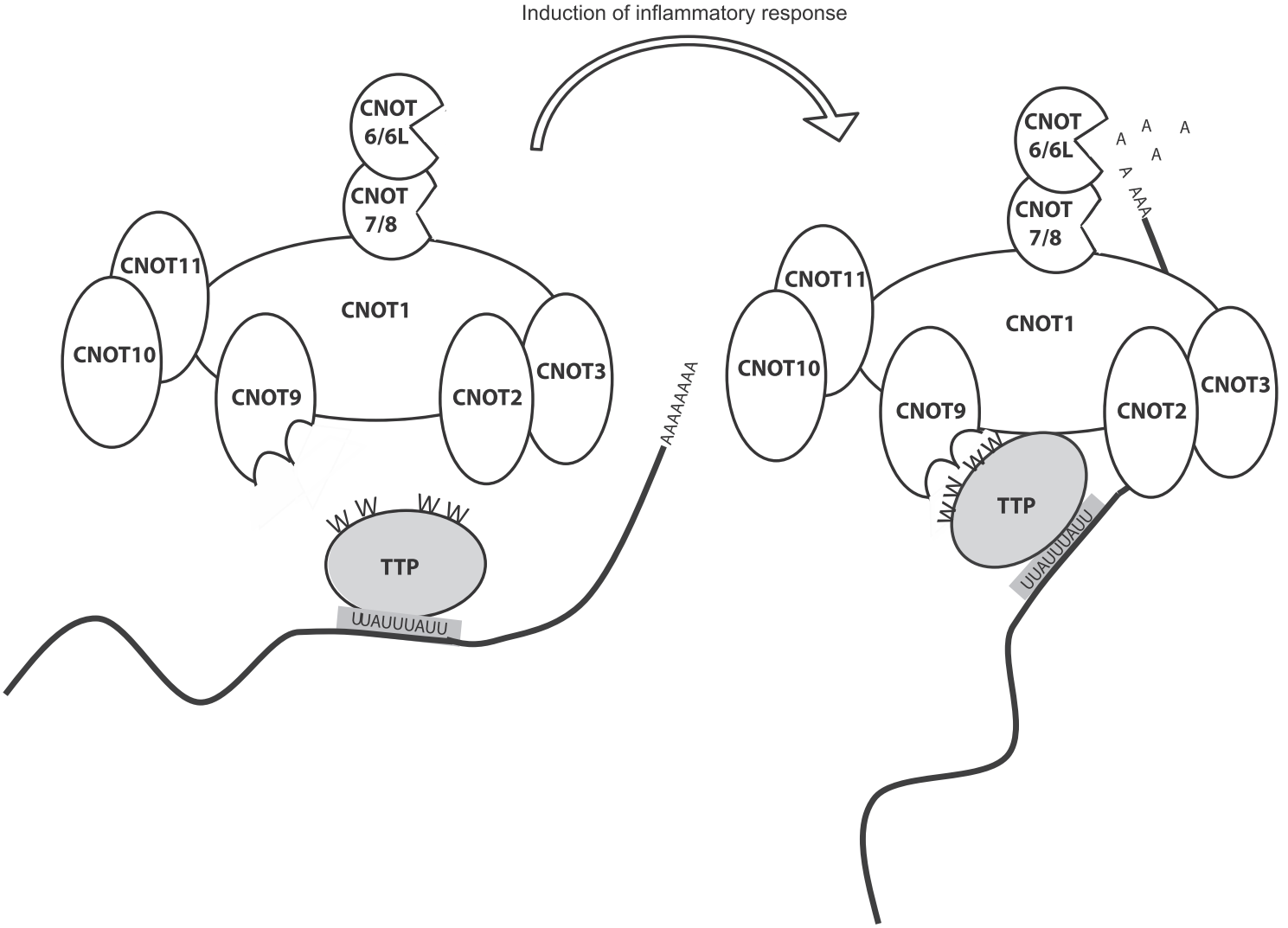

Graphics Abstract

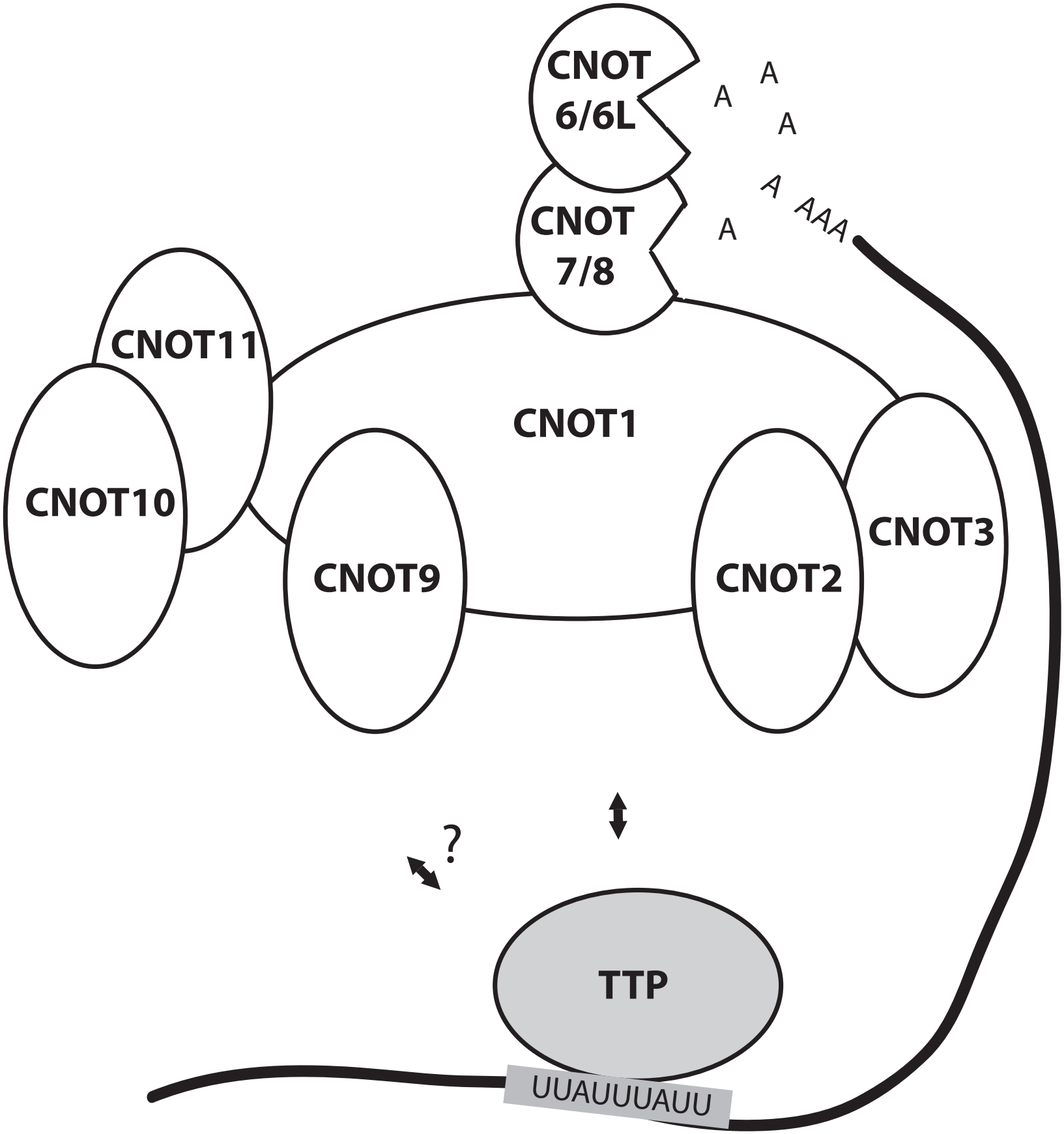
CNOT
6/6L
CNOT
7/8
A
A
A
A
A
AAA
CNOT11
CNOT10
CNOT1
CNOT9
CNOT2
CNOT3
?
TTP
UUAUUUAUU

Figure 1

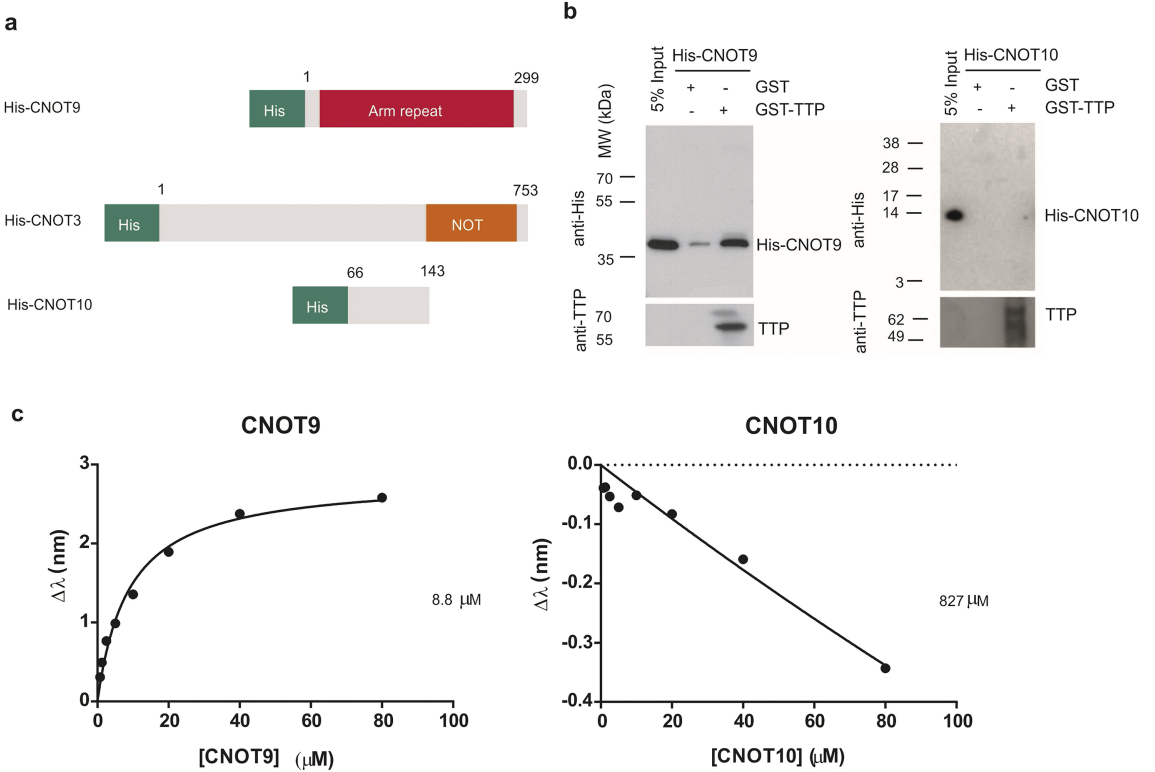
a
His-CNOT9
1
299
His
Arm repeat
His-CNOT3
1
753
His
NOT
His-CNOT10
66
143
His
b
His-CNOT9
5% Input
GST
GST-TTP
MW (kDa)
anti-His
anti-TTP
70
55
35
His-CNOT9
TTP
His-CNOT10
38
28
17
14
3
62
49
c
CNOT9
Δλ (nm)
8.8 μM
[CNOT9] (μM)
CNOT10
827 μM
[CNOT10] (μM)

Figure 2

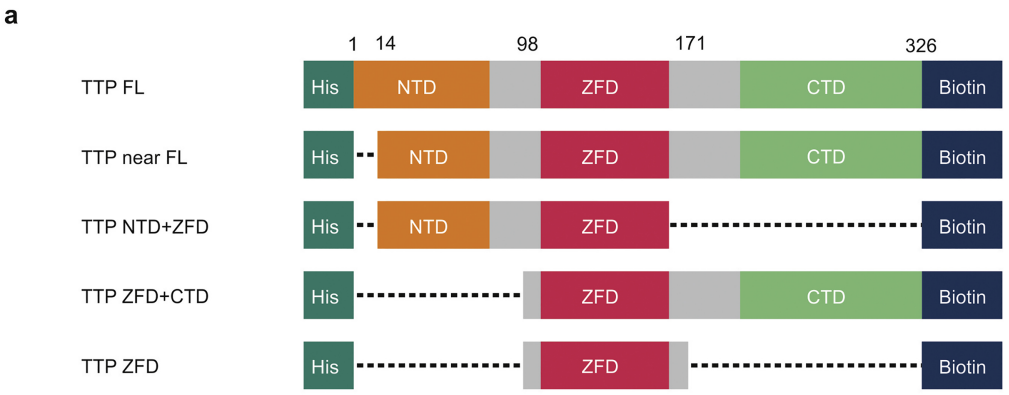

b

Construct	Construct boundaries (aa)	Kd (μM)
TTP near FL	TTP (14-326)	5.5 ± 0.6
TTP NTD+ZFD	TTP (14-171)	5.8 ± 1.2
TTP ZFD+CTD	TTP (98-326)	9.6 ± 1.8
TTP ZFD	TTP (98-171)	17.3 ± 2.4

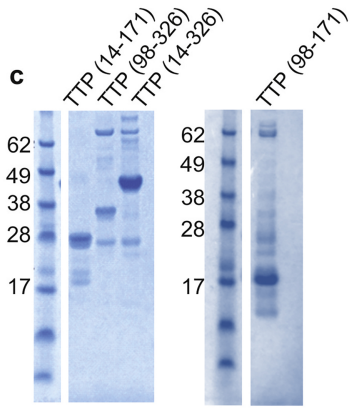

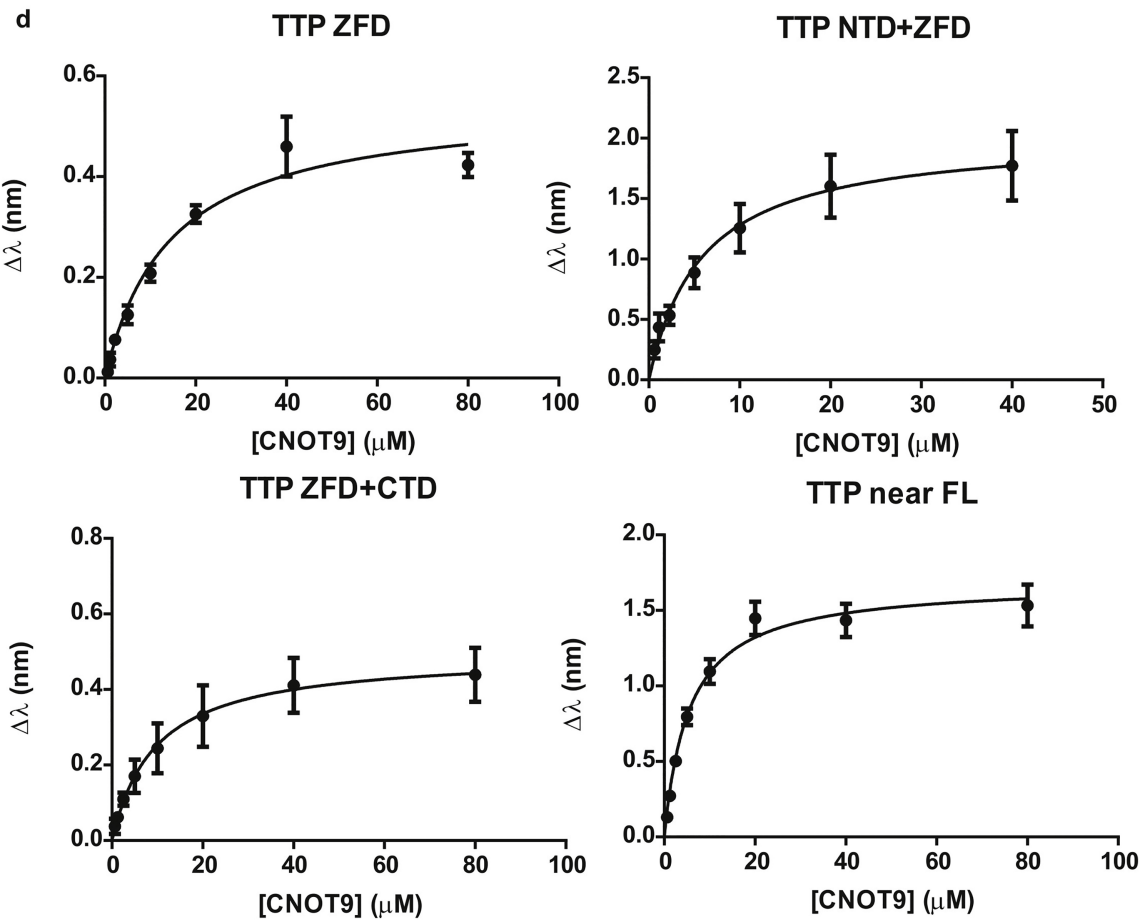

Figure 3

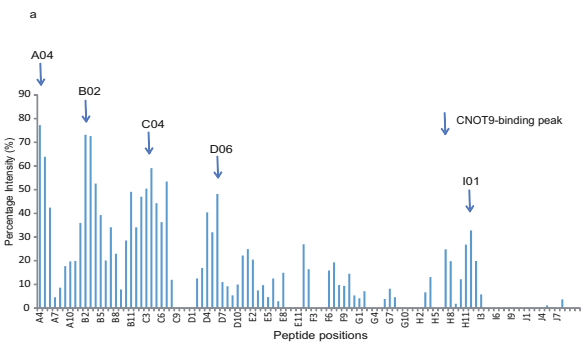

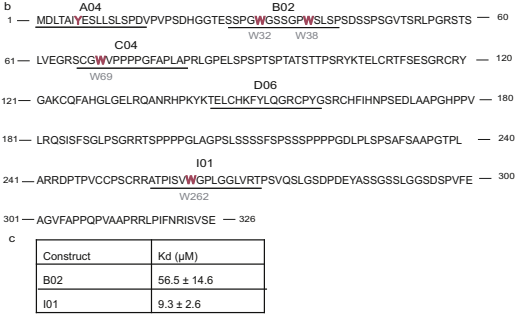

Construct	Kd (μM)
B02	56.5 ± 14.6
I01	9.3 ± 2.6

Figure 4

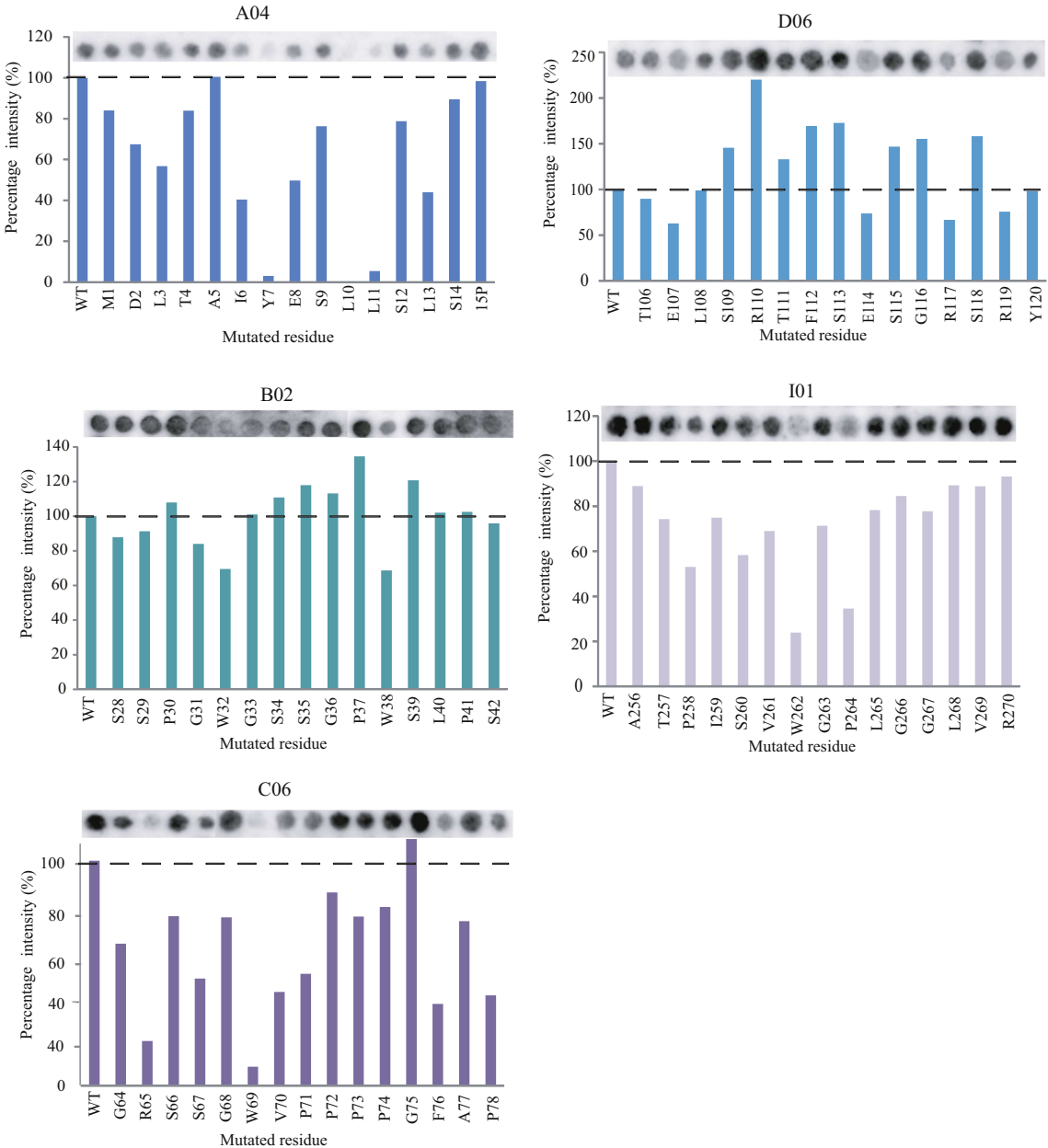
A04
Percentage intensity (%)
120
100
80
60
40
20
0
WT M1 D2 L3 T4 A5 I6 Y7 E8 S9 L10 L11 S12 L13 S14 15P
Mutated residue
D06
Percentage intensity (%)
250
200
150
100
50
0
WT T106 E107 L108 S109 R110 T111 F112 S113 E114 S115 G116 R117 S118 R119 Y120
Mutated residue
B02
Percentage intensity (%)
140
120
100
80
60
40
20
0
WT S28 S29 P30 G31 W32 G33 S34 S35 G36 P37 W38 S39 L40 P41 S42
Mutated residue
I01
Percentage intensity (%)
120
100
80
60
40
20
0
WT A256 T257 P258 I259 S260 V261 W262 G263 P264 L265 G266 G267 L268 V269 R270
Mutated residue
C06
Percentage intensity (%)
100
80
60
40
0
WT G64 R65 S66 S67 G68 W69 V70 P71 P72 P73 P74 G75 F76 A77 P78
Mutated residue

Figure 5

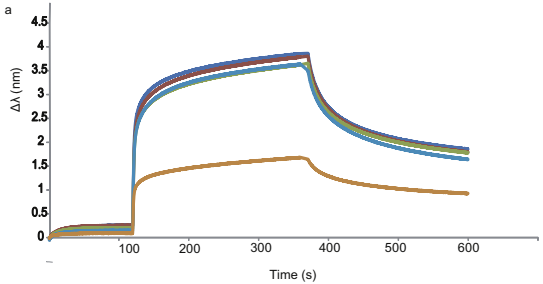

b

Construct	Kd (μM)
TTP wt	10.3 ± 2.1
TTP W32A	9.3 ± 1.9
TTP W38A	10.9 ± 2.3
TTP W262A	11.4 ± 2.9
TTP 4WA	81.4 ± 7.2

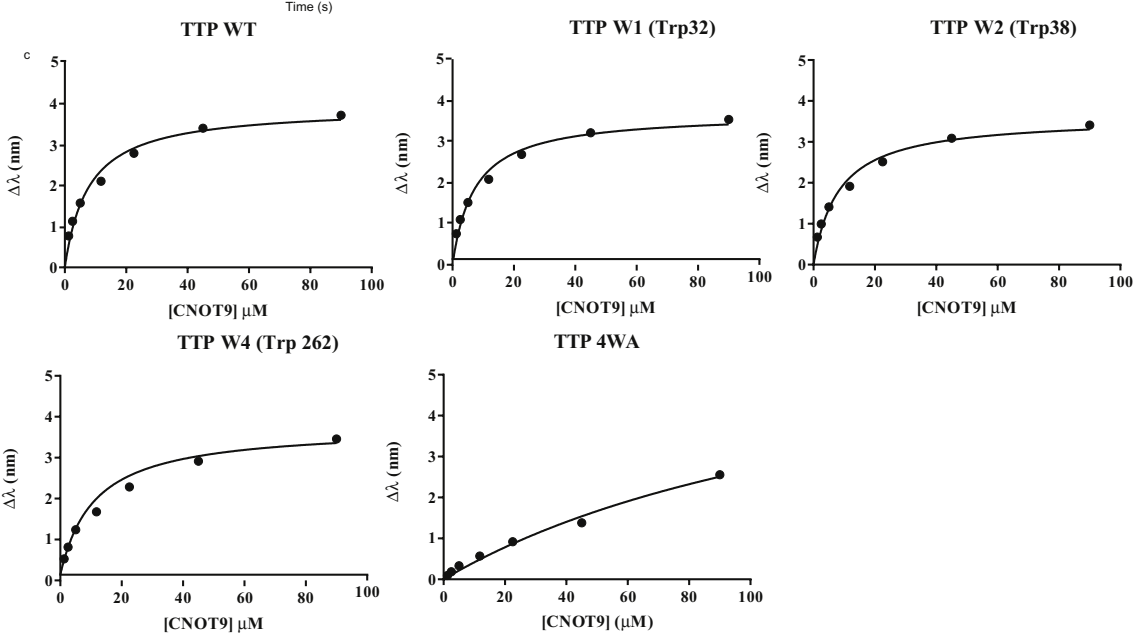

Figure 6

a

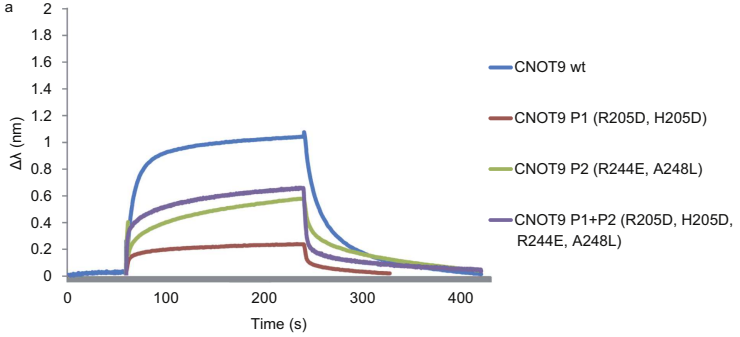

b

Construct	Kd (μM)
CNOT9 wt	8.3 ± 0.7
CNOT9 P1	18.2 ± 4.3
CNOT9 P2	18.3 ± 6.7
CNOT9 P1+P2	23.1 ± 8.4

c

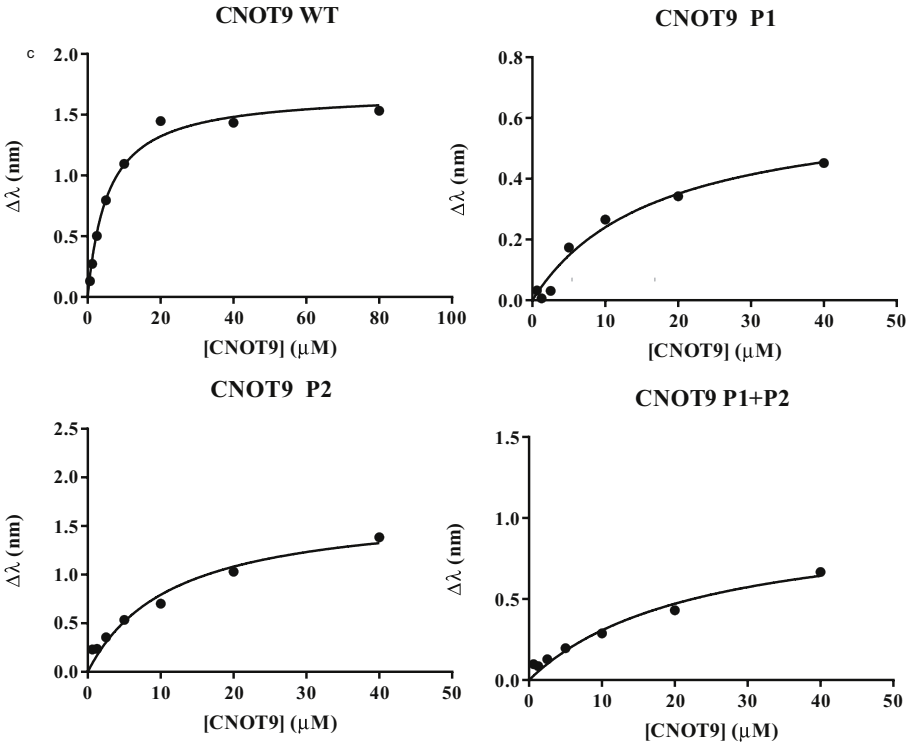

Figure 7

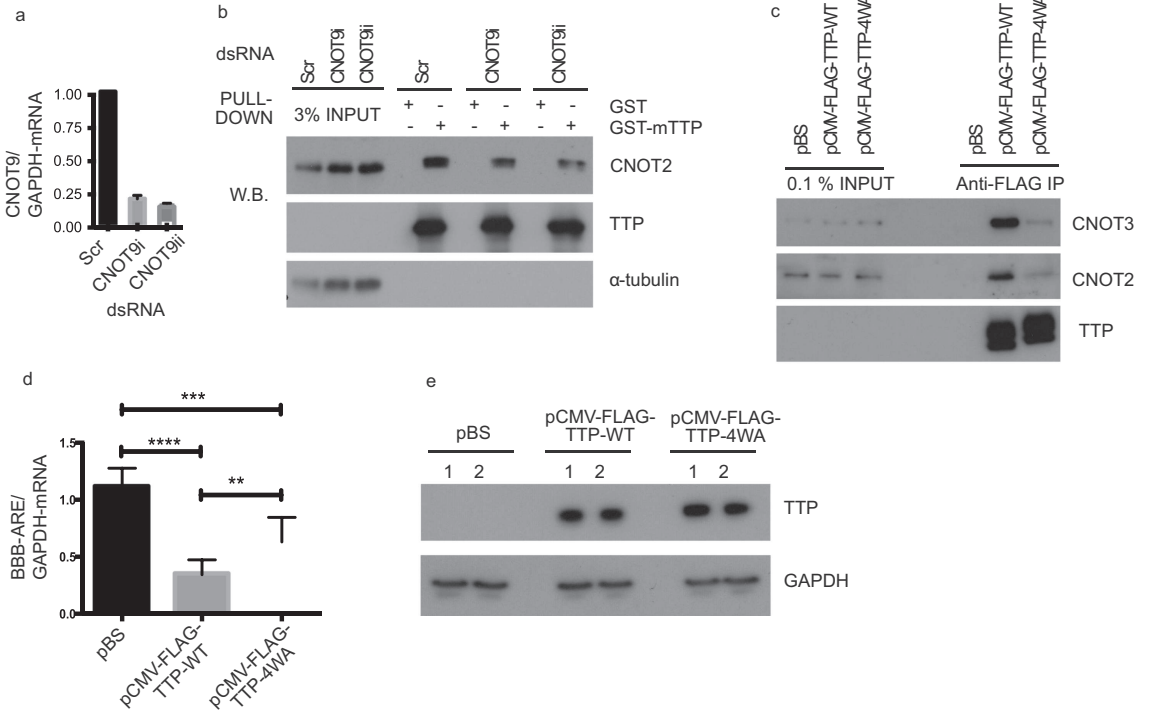
a
CNOT9/ GAPDH-mRNA
1.00
0.75
0.50
0.25
0.00
Scr
CNOT9i
CNOT9ii
dsRNA
b
dsRNA
Scr
CNOT9i
CNOT9ii
Scr
CNOT9i
CNOT9ii
PULL-DOWN
3% INPUT
GST
GST-mTTP
W.B.
CNOT2
TTP
α-tubulin
c
pBS
pCMV-FLAG-TTP-WT
pCMV-FLAG-TTP-4WA
pBS
pCMV-FLAG-TTP-WT
pCMV-FLAG-TTP-4WA
0.1 % INPUT
Anti-FLAG IP
CNOT3
CNOT2
TTP
d
***
****
**
BBB-ARE/ GAPDH-mRNA
1.5
1.0
0.5
0.0
pBS
pCMV-FLAG-TTP-WT
pCMV-FLAG-TTP-4WA
e
pBS
pCMV-FLAG-TTP-WT
pCMV-FLAG-TTP-4WA
1 2
1 2
1 2
TTP
GAPDH

Figure 8